Landscape epidemiology of ash dieback

Marie Grosdidier, Thomas Scordia, Renaud Ioos, Benoit Marçais

Journal of Ecology (2020)
Doi: 10.1111/1365-2745.13383

Landscape epidemiology of ash dieback

Marie Grosdidier[1, 2], Thomas Scordia[3], Renaud Ioos [2], Benoit Marçais [1]

Corresponding author: benoit.marcais@inrae.fr

1 Université de Lorraine - Inrae, UMR Interactions Arbres/Microorganismes, 54000, Nancy, France

2 ANSES Laboratoire de la Santé des Végétaux, Unité de Mycologie, Domaine de Pixérécourt, Bâtiment E, 54220 Malzéville, France

3 Département de la Santé des Forêts Auvergne-Rhône-Alpes, Ministère de l'agriculture et de l'alimentation DGAL-SDQPV, 251 rue de Vaugirard, 75732, Paris, France

Abstract

1. Ash dieback is induced by *Hymenoscyphus fraxineus*, an invasive pathogenic fungus. It is causing severe damage to European ash populations. However, the local environment, such as climate or site conditions, is known to affects ash dieback.
2. We studied the landscape epidemiology of the disease on a 22 km² area in north-eastern France at two stages of the invasion process using Bayesian spatio-temporal models fitted with integrated nested Laplace approximation (INLA). Several features characterizing disease severity, crown dieback, frequency of collar canker, and density of infected leaf debris in the litter were determined on a regular grid over a 3.5 x 6.5 km area. We first analysed the effect of landscape features on the disease establishment stage in 2012, two years after the first report of the disease in the area, and then on further disease development, in 2016-2018.
3. Landscape features had little impact on the disease at the establishment stage, but strongly determined its further development. Local fragmentation of tree cover was the most important factor, with trees that are isolated or in hedges far less affected than trees in a forest environment. We showed that they were subjected to different microclimates, with higher crown temperatures unfavourable to pathogen development. Low host density strongly reduced disease development. The presence of large ash populations in the vicinity affected local disease severity up to several hundred meters.
4. **Synthesis.** We showed that the landscape characteristics strongly affect the development and spread of ash dieback. The disease is far less severe in forest conditions when ash density is low or in open canopies such as hedges and isolated trees. Ash trees are often in these types of landscapes, which should strongly limit the overall impact of Ash dieback.

Key words: Fraxinus, *Hymenoscyphus fraxineus*, invasion, disease emergence, disease spread, disease severity,

Introduction

Ecologists have studied the interaction between spatial patterns and ecological processes in a landscape context since the 1960s (Turner, 2005). However, this research approach has not been used broadly in plant pathology, although interest in landscape epidemiology has developed over the last decade (Plantegenest, Le May & Fabre, 2007; Meentemeyer, Haas & Václavík, 2012). It has been increasingly recognized that landscape features are important for pathogen spread, establishment and persistence in spatially structured host populations (Hutchinson & Vankat, 1998; Krewenka *et al*., 2011; Kelly &

Meentemeyer, 2002). Landscape epidemiology aims to determine how these mechanisms shape disease severity (Plantegenest, Le May & Fabre, 2007). The spatial arrangement and composition of host vegetation is especially important for pathogens affecting long-lived hosts such as forest trees (Condeso & Meentemeyer, 2007). For example, Perkins and Matlack (2002) suggested that the emergence of fusiform rust on pines in the south-eastern United States might have been promoted by a human-induced change of the landscape, with larger patches of hosts more favourable to disease development. Rodewald and Arcese (2016) stressed the importance of landscape features in promoting or hampering the dispersal of invasive species. Roads or water courses can act as corridors for invasive species such as *Phytophthora* spp. because the propagules are dispersed by contaminated water or soil (Jung & Blaschke, 2004; Jules *et al*., 2002). Infected fallen leaves can also be dispersed by vehicles as shown for the horse chestnut leafminer *Cameraria ohridella* (Guichard & Augustin, 2002). Microclimate conditions that affect pathogen reproduction and survival are often determined by landscape patterns (Condeso & Meentemeyer, 2007; Kelly & Meentemeyer, 2002). In this way, topographic, edaphic, climatic, vegetation and historical landscape features can play a key role in disease expression, and are often critical in the spread of invasive pathogens.

The relationship between disease spread/severity and landscape may be studied at several spatial and temporal scales using either static or dynamic models to respond to different questions, such as inference or prediction. In order to do this, specific tools have been developed that enable data analysis with spatial and temporal dependence. A method used more and more commonly , the Bayesian space-time modelling approach with integrated nested Laplace approximation (INLA) is now widely available in R package software (R Core Team, 2019). This tool has been used to analyse the effect of host structure or environment on disease presence or severity (Schrödle & Held, 2011; Marçais et al., 2016).

Ash dieback is an emerging disease induced by an invasive pathogen, *Hymenoscyphus fraxineus,* and has been severely damaging European ash stands since the late 1990s (*Fraxinus excelsior* and *F. angustifolia*). The fungus induces foliar infections, shoot blight, and collar cankers that often lead to tree death (Marçais *et al.*, 2017). Originating from Asia, it was first reported in Poland in the 1990s and spread across Europe to reach France in 2008. The biological cycle of *H. fraxineus* takes one year (Gross *et al.,* 2014). Ash leaves are infected during the summer by airborne ascospores. At the end of the summer, the pathogen extends from the leaves to the stem, inducing shoot mortality and significant crown dieback. The pathogen then overwinters in the leaf rachis (petiole + main leaf vein) in the forest litter. Apothecia develop on the infected rachides and release ascospores in June-August. This disease has been reported to threaten European ash populations, and it has been stressed that understanding how the landscape might influence disease development and spread as well as management strategies is of critical importance (Pautasso *et al.*, 2013).

Several environmental factors, such as site moisture, temperature, stand age, and stocking density that reflects canopy closure, are known to influence disease severity (Skovsgaard *et al.,* 2017). Reports on the impact of host density on disease severity have been conflicting (Skovsgaard *et al.,* 2017). Nevertheless, it is clear that dense stands with a closed canopy are highly susceptible to the fungus, while ashes in open habitats or near forest edges appear to be less affected (Havrdová & Cerný 2013; Rosenvald *et al.,* 2015; Vacek *et al.,* 2015). *Hymenoscyphus fraxineus* has also been shown to have poor survival at temperatures above 35°C, which affects the disease epidemiology (Hauptman *et al.,* 2013, Grosdidier *et al.*, 2018). The fungus also needs high moisture to develop, with moist sites deteriorating faster and showing more frequent canker at the trunk base (*Husson et al.,* 2012; Vacek *et al.,* 2015; Marçais *et al.,* 2016; Havrdová *et al.,* 2017).

Landscape features could impact disease severity through multiple mechanisms, by promoting its spread (dispersal of infected rachides by road or river), affecting micro-climatic conditions important for its development or survival, or through the density of ash hosts in the neighbourhood. To test these hypotheses, a landscape survey was carried out on an area of approximately 22 km² at different stages of disease development, either shortly after disease

arrival or after several years of disease development. The effects of the environment on crown dieback severity, collar canker, and abundance of infected rachides in the litter were analysed in the framework of Bayesian hierarchical modelling.

Materials and Methods

Sampling area

A study area of approximately 3.5 x 6.5 km was established around the village of Champenoux, in north-eastern France, 15 km from the city of Nancy (Lorraine region), to encompass both forest and agricultural settings with scattered hedges and small woods in equal proportions. *Fraxinus excelsior* L. is the only ash species present in the area. After the first report of ash dieback in France in 2008, five locations within the study area were surveyed annually including the only ash plantation present in the area, where *H. fraxineus* might have been introduced by planting infected material. Ash dieback was observed for the first time in 2010 on a few trees at each of two points close to the road.

Plots with a radius of 25 m were established on each node of a grid including 799 nodes. The grid was 200 x 200 m in the forested area, and 141 x 141 m in agricultural settings, to avoid over-representing forest locations in the dataset (Fig. S1). A preliminary survey was done based on aerial photography to check for the presence of trees on the nodes. A ground survey was then carried out in 2012 on nodes with tree presence to check for the presence of ashes, and to characterize the node environment. The number and size of ashes present on a 25 m radius plot was recorded, as well as the presence of ash dieback. At that stage, infected shoots were sampled for analysis on 1-3 symptomatic ashes per studied plot. The samples were analysed by qPCR for the presence of *H. fraxineus* as described in Ioos *et al.* (2009).

A plot was set out at all nodes with the presence of at least five ashes, irrespective of the size, which altogether represented 127 of the 799 nodes (Fig. 1).

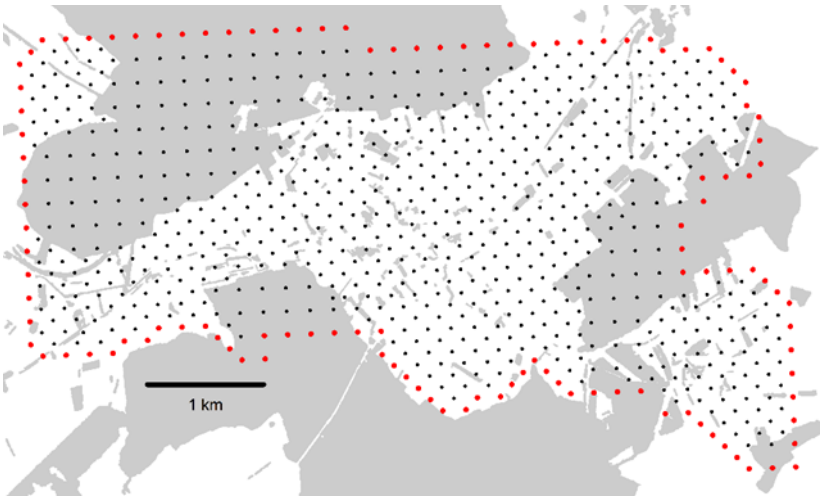

Fig S1. Study area map. Black dot, grid points where ash dieback was characterized, red dot, grid points where only ash basal area was measured to minimize the border effect. The grid density is twice in the non-forest area to limit the over-representation of forest. The grey area is the area with tree cover.

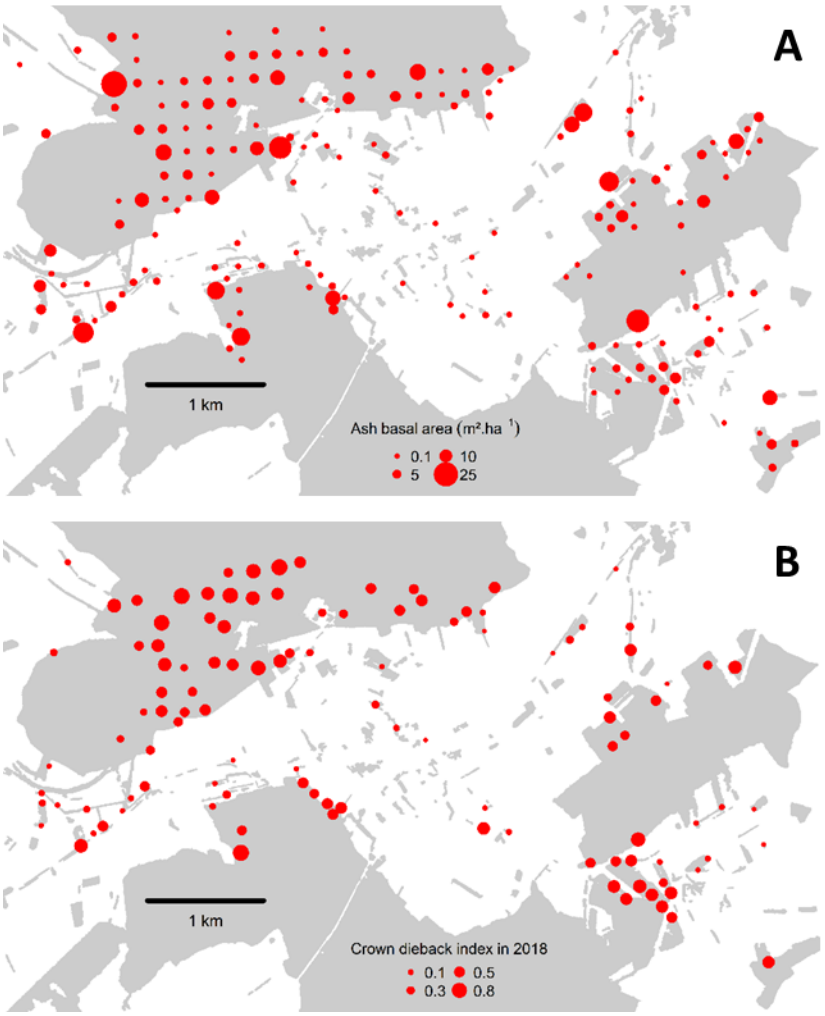

Fig. 1. Plot spatial distribution in the studied area. (A) Host density (Ash dieback parameters were not studied in plots at the edge of the area), (B) Crown dieback index in 2018. The greyed area represents the tree cover, with large tracks of forested area in the north and south of the area.

Environmental characteristics of plots

In all, 80 plots were set up in the forested area, while 47 were in an urban or agricultural environment. An index of tree cover fragmentation was computed from a tree cover shape file, which was corrected when needed from aerial photographs taken in 2015. Both the tree cover shape file and aerial photographs were retrieved form the IGN site (http://professionnels.ign.fr). The polygons of tree cover within a radius of 100 m from each plot were extracted, and the perimeter-to-area ratios of these polygons were computed as an index measuring to what degree trees were isolated or within a tree stand. The distances of each plot from the road (either coated road or dirt road), river and forest edge were computed using QGIS software and IGN aerial photographs. Computations were done in R software, using the rgdal, rgeos and geosphere packages.

The basal area of ash present at each of the 127 plots was also characterized as a measure of host density (Fig. 1a). Three concentric squares centred on the plot were set up with a diagonal of 16, 40 and 50 m oriented in cardinal directions (128, 800 and 1250 m²). Ash trees were sampled depending on their diameter at breast height (dbh, at 1.3m from soil line). Ashes of dbh 2.5 – 22.6 cm were measured in the 128 m² square, those of dbh 22.6 – 37.6 cm in the 800 m² square, and those of dbh over 37.6 cm in the 1250 m² square. For each site, the

ash basal area per ha was computed. To avoid over-estimating the basal area in areas with small woods, hedges or isolated trees, the total basal area was weighted by the proportion of tree cover within 100 m from the plot. The ash basal area at nodes with too few trees to establish a plot (less than five) was estimated using the initial count and dbh estimation of the ash trees present within the 25 m radius circle.

Crown temperatures vs. forest environment

EL-USB-2 temperature sensor/data loggers (Lascar Electronics Ltd UK, Wiltshire, United Kingdom) were set up in the crown of 16 ashes between July 9 and September 12, 2016. They were placed with a slingshot approximately in the middle of the crown and on the east side. Temperatures and relative humidity were measured each hour. Eight ashes were isolated trees in agricultural settings, while eight others were in forest stands to study the influence of canopy closure on crown microclimatic conditions. The heights of the sensors and of the top and bottom of the crown were determined. Hourly temperature data were extracted from the Météo-France station of Champenoux (WGS84 E 48.751 N 6.340) in 2016.

Crown temperatures measured by the data logger were modelled by a linear model, depending on temperatures measured at the meteorological station and at the tree location (forest stand/isolated tree). Hours were added as a factor in the linear model to take into account hourly variability in each day measured. In order to investigate the possible influence of the heat wave that occurred in Eastern France in 2015, averages of maximum daily temperatures inferred by the model in 2015-17 were used for further analysis. We computed for each year the number of hours where crown temperatures reached values above 35°C.

Disease measurement

The first assessment of disease severity was carried out in June-July 2012, two years after the first report of Ash dieback in the area (hereafter referred to as the disease establishment stage). Three additional disease assessments were conducted in June 2016, 2017 and 2018. As the initial spread of *H. fraxineus* within the studied area appeared to have been extremely rapid, the environment was thought to be the main driver of disease severity, as ash dieback had been present throughout the area for at least 5-7 years (hereafter referred to as the disease development stage). Ash crowns were rated according to six dieback scores: 0 for no dieback, 0.05 for 1 to 10% dieback, 0.35 for 10 to 50% dieback, 0.625 for 50 to 75% dieback, and 0.875 for 75 to 99% dieback or tree with stem dead and sprout at the stem base, 1 for dead trees. A crown dieback index was computed for each plot by averaging the dieback score of all ashes at the plot. Presence or absence of canker at the trunk base was also rated for each of the studied trees. To minimize border effects, plots located at the edge of the studied area were characterized for the environment and the host density, but not for ash dieback parameters. Depending on the year, 100 to 114 plots were rated, some plots being abandoned because no ashes remained present, while others were added because of ash recruitment.

To better characterize inoculum sources, the density of ash rachis in the litter was determined for each of the studied plots in May 2016, and again from March to May 2017. To do this, rachides were sampled along transects consisting of 0.1 x 10 m strips located at the plot center. In 2016, one transect was sampled per plot. In 2017, two perpendicular transects intersecting in their middle were sampled; rachides were sampled for 1 m sections separated by 1 m along each of the two transects. The rachides were sorted in the laboratory into two categories: either infected, i.e. black rachis with presence of a pseudosclerotial plate, or healthy, i.e. white or beige rachis without any pseudosclerotial plate. In 2016, we determined the length of rachis in each of these two categories. In 2017, the dry weight in each of the two categories was determined after 48 hours in a heat chamber at 50°C. The density of rachides in the litter for each category was computed in $m.m^{-2}$ using a linear equation between the two measurements established in 2016 (L = 163.73*DW, with L, the length in cm and DW, the dry

weights of rachides (Grosdidier, unpublished results). The validity of the rachis infection assessment was checked in 2016 by a fructification test. Infected and non-infected rachides were sampled (20 of each per plot on 28 plots) and placed in laboratory conditions in a wet chamber at 20°C for about one month, to assess their ability to produce *H. fraxineus* apothecia.

Additionally, infected rachides were harvested in the litter in August along 3 strips of 1 x 0.1 m each in 23 plots in 2016, and 31 in 2017. Eleven plots were visited in both years. The length of infected rachides was measured as previously described and the number of apothecia present on each of them was counted. The number of apothecia per cm of infected rachis was then determined. The sampled plots were selected to cover the available range of tree cover fragmentation and distance to the river. The log-transformed number of apothecia per cm of infected rachis was analysed by regression using the year, tree cover fragmentation, and the log of distance to the river, as independent variables.

Table S1 shows an overview of all measures taken.

Statistical analysis

Statistical analyses were conducted separately for the disease establishment (2012 data) and development stages (2016-18 data).

Analyses were performed using the "INLA" R package to account for the spatial and temporal dependencies. The response variable y_{it} was either the mean proportion of crown dieback, the proportion of trees with collar canker, the proportion or the density of infected rachides in the litter at plot s_i $(i = 1, \dots, n)$ and in year $t = 1, \dots, T$. To analyse the crown dieback index, which corresponds to proportions not based on the number of cases observed, a $Beta\ (\eta_{it}, \sigma_e^2)$ distribution was used. For the collar canker prevalence or the proportion of infected rachides, a $Binomial\ (\eta_{it}, \sigma_e^2)$ distribution was assumed. Lastly, the density of infected rachides in the litter was log transformed and analysed with a $Normal\ (\eta_{it}, \sigma_e^2)$distribution. σ_e^2 represents the variance of the measurement error defined by a Gaussian white noise process, both serially and spatially uncorrelated, and $f(\eta_{it}) = b_0 + \sum_{m=1}^{M} \beta_m x_{mi} + \omega_{it}$, where b_0 is the intercept, and $\beta_{1,\dots,}\beta_M$ are the fixed effects related to covariates $x_{1,\dots,}x_M$. The link function f used was the logit function for the mean proportion of crown dieback, the proportion of trees with collar canker, and the proportion of infected rachides in the litter and the identity function for the density of infected rachides in the litter. The term ω_{it} refers to the latent spatio-temporal process which changes in time with first-order autoregressive dynamics and spatially correlated innovations: $\omega_{it} = a\omega_{i(t-1)} + \sqrt{(1-a^2)}\xi_{it}$, with $t = 2, \dots, T$, $|a| < 1$ and $\omega_{it}, \xi\_\{it\} \sim Normal(0, \sigma^2)$. Moreover, ξ_{it} is a zero-mean Gaussian field, assumed to be temporally independent and characterized by the following spatio-temporal covariance function: $Cov(\xi_{it}, \xi_{ju}) = \begin{cases} 0 & if \quad t \neq u \\ Cov(\xi_i, \xi_j) & if \quad t = u \end{cases}$ for $i \neq j$, where $Cov(\xi_i, \xi_j)$ is given by a Matérn spatial covariance function defined by $Cov(\xi_{it}, \xi_{ju}) = \frac{\sigma^2}{\Gamma(\lambda)2^{\lambda-1}}(\kappa\|i-j\|)^{\lambda}K_{\lambda}(\kappa\|i-j\|)$, where $\|i-j\|$ is the Euclidean distance between two generic locations and σ^2 is the marginal variance. K_{λ} denotes the modified Bessel function of the second kind and order $\lambda > 0$, where the smoothness parameter λ of the process is usually kept fixed due to poor identifiability. Conversely, $\kappa > 0$ is a scaling parameter related to the range $\rho = \frac{\sqrt{8\lambda}}{\kappa}$ which corresponds to the distance at which the spatial correlation is close to 0.1, for each $\lambda \geq \frac{1}{2}$. A mesh for the spatial domain was first created.

Analysis at the disease establishment stage was carried out with no temporal variation in the spatial field (i.e., by setting a=1). Thus, term ω_{it} corresponds only to ξ_{it} with t = 2012. For analysis at the development stage, the full spatio-temporal model was compared to simplified versions of the model: (i) a spatial model only with no first-order autoregressive dependency between years (such that a=0, and ω_{it} is equal to ξ_{it} for t = 1 for 2016, 2 for 2017

and 3 for 2018); (ii) a temporal model only, with no spatial dependency; (iii) a spatio-temporal model with independent spatial and temporal effects. Models were compared using the deviance information criterion (DIC). The model with the lowest DIC was chosen to assess for effect of covariates.

In a preliminary step, the range at which host density might impact ash dieback was studied. The hypothesis was that host patches might enhance disease development depending on their host basal area and their distance from the focal point. Two kernels were tested to determine how this influence may decay with distance, the exponential and the Epanechnikof kernel, using ranges of 0, 100, 200, 300, 400 and 500. The host abundance in the neighbourhood of a plot i (HAN_i) was then computed as $\sum_{m=1}^{M} K(Dim)BAm$ with BA_m, the ash basal area at plot m; D_m, the distance between plot i and m; and K, the selected kernel. To account for a density of the grid that was twice in agricultural settings, BA_m, the ash basal area in neighbouring plot m located in agricultural settings was divided by 2. Full spatial models were then fitted using these computed host abundances in the neighbourhoodd with 2018 data only, and the best kernel and appropriate range were selected according to the DIC. This variable HAN was then used as a measure of local host density.

Full spatial/spatio-temporal models were built with a forward strategy for entering variables in the model. Covariates selected for entry were those with fitted parameters with 2.5% and 97.5% quantile ranges that did not span zero and yielding the lower DIC.

Results

Site characteristics and *H. fraxineus* presence

Altogether, depending on mortality, logging and recruitment of ashes during the study period, 100 plots were observed in 2012 and 2016, 109 in 2017, and 111 in 2018. Most of the plots were located in a forest environment, with 67 plots in forest settings and 44 in agricultural ones in 2018. However, many plots had intermediate conditions, being either located at forest edges or in small woods within agricultural settings (15 forest plots and 16 plots in agricultural settings in 2018). To account for this, we used the tree cover fragmentation index that was clearly higher in agricultural settings (0.153 ± 0.019) than in forests settings (0.028 ± 0.003). Ash basal area was significantly higher in forest than in agricultural settings (*p*-value < 0.01, Fig.1a), with mean values of ash basal area of 6.1 ± 1.2 $m^2.ha^{-1}$ in forest and 3.3 ± 1.2 $m^2.ha^{-1}$ in agricultural settings. Only two pure ash stands were present in forest environments in the area. Ash was usually at low density in stands mixed with oaks (*Quercus robur* L.and *Q. petraea* L.) and hornbeam (*Carpinus betulus* L.). By contrast, small woods in agricultural settings, although limited in size, were often pure ash stands.

In 2012, only two years after disease arrival in the village of Champenoux, ash dieback was observed in all studied plots with 74% of the ashes showing at least limited disease symptoms, and 47% of them showing moderate to severe crown decline. The mean crown dieback index was 28 ± 3%. *Hymenoscyphus fraxineus* could be identified by qPCR from 93% of the plots sampled (n= 120, including border nodes and plots with less than five ashes). The plots where *H. fraxineus* could not be detected by qPCR were stands with 1-3 large ash trees, where adequate samples were difficult to collect. Nevertheless, only six trees among the 1424 trees observed in 2012 showed presence of collar canker. In 2016, four years later, the disease had increased in severity (Fig. 2a, b). The mean crown dieback indexes observed in 2016, 2017 and 2018 were 36 ± 3, 33 ± 3 and 40 ± 4%, respectively. Collar cankers were observed on 231, 229 and 294 trees in 2016, 2017 and 2018, respectively (16%, 18.4% and 25.1%).

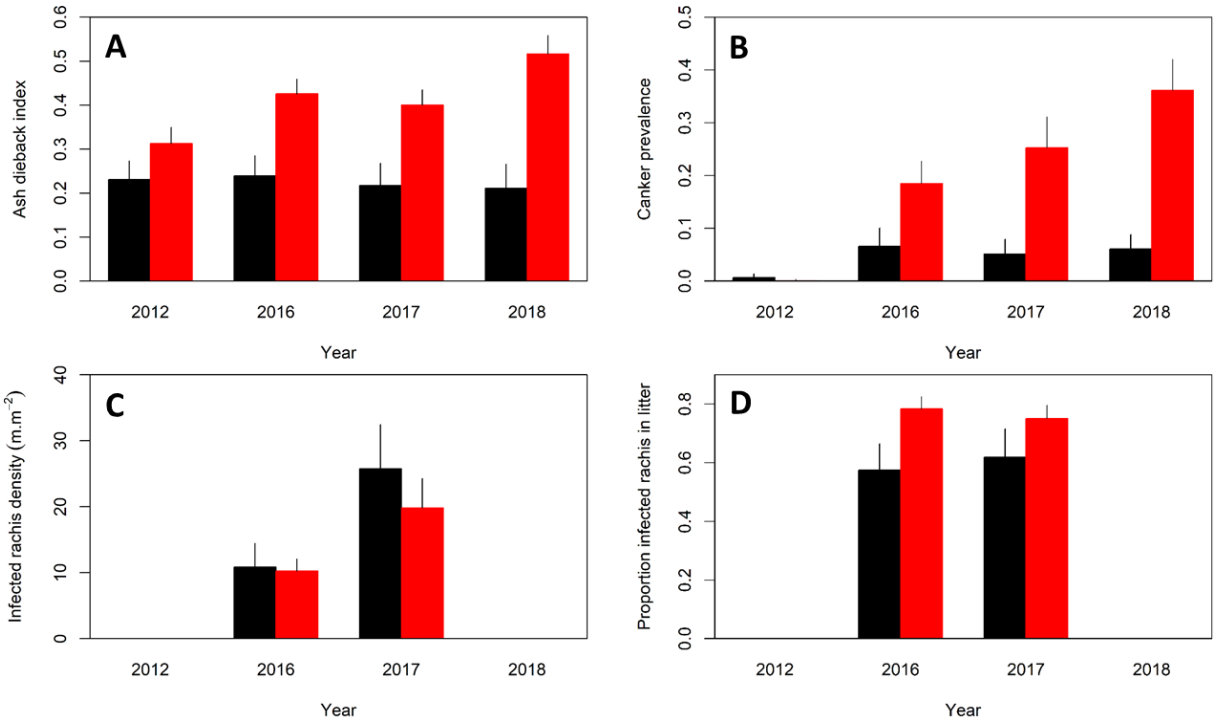

Fig. 2. Evolution of ash dieback on the studied plots from 2012 to 2018. A. Ash dieback index (proportion of shoot mortality), B. Collar canker prevalence, C. Density of ash rachides infected by *H. fraxineus* in the litter, D. Proportion of ash rachides in the litter that are infected by *H. fraxineus*. Black bar: agricultural settings: Red bar, forest settings. Data on ash rachis status and density in the litter (C, D) are available only in 2016-17.

Effect of the landscape on ash dieback, collar canker and rachis infection

In a preliminary step, the range at which host density might impact crown dieback was studied. The host abundance in the neighbourhood (HAN) computed using an exponential kernel with a range of 200 m, yielded the lower deviance information criteria (DIC) for both the 2018 ash dieback index and basal canker prevalence (Fig. 3). Respective DIC values were -128.7 and 355.9 compared to -116.5 and 363.2 for the plot ash basal area. Using the Epanechnikof kernel to compute the HAN yielded slightly larger DIC values.

Disease establishment stage (2012)

The analysis at the establishment stage of the disease was done only for the crown dieback index, collar cankers being very infrequent. The only variables that showed a significant relationship with the crown dieback index in 2012 were tree size (dbh) and tree cover fragmentation (Table 1). The dieback index decreased with tree cover fragmentation and with tree dbh, smaller ashes being more severely affected. Ashes in closed canopies were more severely affected than ashes in hedges or isolated ashes. Hence, since 2002, crown decline was less severe in agricultural settings, where tree cover is more fragmented, compared to forest (Fig. 2a). At that stage, dieback severity was not linked to host abundance (HAN) and proximity of the plot to a river or road (Table 1). The estimated range of the spatial dependency in crown decline was 542 m. The spatial field explained some variability in the data that was not taken into account by covariates (Fig. 5).

Table 1: Effects of landscape features on ash crown dieback at the arrival and development stages of the disease. This table shows an estimation of parameter covariates with significant values in bold (those with the confidence interval not containing 0).

Variable[a]	**Establishment stage (2012)**		**Development stage (2016 – 18)**	
	Mean (sd)	**P2.5; P97.5**	**Mean (sd)**	**P2.5; P97.5**
Host abundance in neighbourhood (HAN)	0.01 (0.01)	-0.01; 0.03	**0.04 (0.01)**	0.02; 0.06
Tree cover fragmentation	**-2.64 (1.14)**	-4.96; -0.46	**-7.04 (1.12)**	-9.24; -4.84
Trees size (dbh)	**-0.02 (0.01)**	-0.04; -0.01	**-0.02 (0.004)**	-0.03; -0.01
log(Distance to river)	-0.03 (0.05)	-0.13; 0.08	**-0.13 (0.04)**	-0.20; -0.05
log(Distance to road)	-0.04 (0.05)	-0.13; 0.05	0.04 (0.03)	-0.10; 0.04
σ_e^2	0.116 (0.018)	0.009; 0.158	0.057 (0.007)	0.045; 0.071
κ	0.010 (0.011)	0.002; 0.004	0.005 (0.002)	0.002; 0.009
σ^2	0.030 (0.040)	0.001; 0.143	0.516 (0.158)	0.276; 0.892
ρ	542 (356)	69; 1374	645 (228)	302; 1189
DIC Null model	-103.6		-466.1	
Full model	-110.9		-508.1	

[a] Host abundance in neighbourhood, sum of ash basal area in neighbouring plots weighted by the exponential kernel with a parameter of 200, Tree cover fragmentation, Perimeter-to-area ratio of tree cover within 100 m.

Table 2: Effects of landscape features on prevalence of collar canker and % infected rachides in the litter at the development stage of the disease (2016 – 2018). This table shows an estimation of parameter covariates with significant values in bold (those with the confidence interval not containing 0).

Variable[a]	Prevalence of collar canker		% infected rachides in litter	
	Mean (sd)	P2.5; P97.5	Mean (sd)	P2.5; P97.5
Host abundance in neighbourhood (HAN)	**0.06 (0.02)**	0.03; 0.10	**0.05 (0.01)**	0.02; 0.08
Tree cover fragmentation	**-7.53 (2.46)**	-12.36; -2.71	-0.92 (2.12)	-5.09; 3.25
Trees size (dbh)	0.01 (0.01)	-0.01; 0.03	-0.012 (0.008)	-0.03; 0.01
log(Distance to river)	-0.002 (0.08)	-0.17; 0.16	**-0.23 (0.06)**	-0.51; -0.11
log(Distance to road)	**0.135 (0.07)**	0.01; 0.27	0.03 (0.06)	-0.09; 0.14
σ_e^2	0.327 (0.048)	0.257; 0.445	0.366 (0.057)	0.286; 0.509
κ	0.008 (0.002)	0.004; 0.014	0.009 (0.003)	0.005; 0.015
σ^2	3.027 (0.933)	1.678; 5.313	4.382 (1.241)	2.575; 7.411
ρ	403 (117)	208; 664	352 (97)	185; 560
DIC Null model	1050.0		987.0	
Full model	1029.4		973.1	

[a] Host abundance in neighbourhood, sum of ash basal area in neighbouring plots weighted by the exponential kernel with a parameter of 200, Tree cover fragmentation, Perimeter-to-area ratio of tree cover within 100 m.

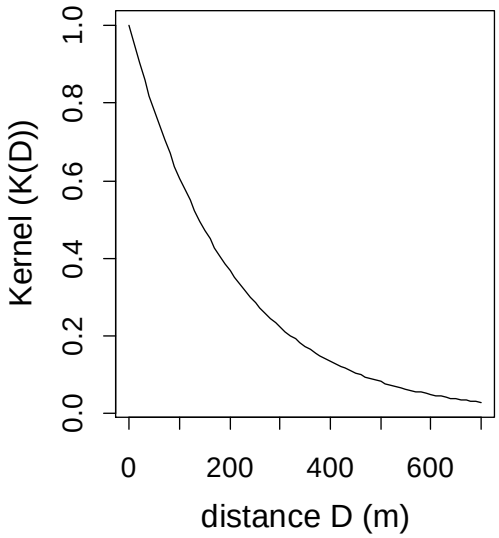

Fig. 3. Decay with distance of influence of the host abundance in the neighbourhood on ash dieback. The best kernel was the exponential kernel with a range of 200 (K(G) = exp(-D / 200)).

Disease development stage (2016-18)

Models without covariates with only a spatial effect, a temporal effect, both a spatial and a temporal effect without time * space interactions were compared to the full spatio-temporal model. For the crown dieback index, the respective DIC values were -445.7, -151.7, -463.5 and -466.0, indicating that the model with time, spatial effects and their interactions had a better fit, although the time * space interactions provided only a small improvement. The same results were obtained with canker prevalence and proportion of rachis infected (result not shown). Spatio-temporal models with interaction between spatial and temporal effects were thus chosen for further analysis.

Ash dieback was strongly influenced by landscape at the development stage. Tree cover fragmentation, ash abundance in the neighbourhood (HAN) and distance to the river were all significantly related to both the crown dieback index and collar canker prevalence (Table 1 and 2). As during the establishment stage, ashes located in plots with a higher tree cover fragmentation index were far less affected by ash dieback (Fig. 1b, Fig. 4a). Strikingly, the disease increased in severity with time in forest conditions but not in agricultural settings, where tree cover was highly fragmented (Fig. 2 a, b). Ash dieback severity strongly increased with HAN (Fig. 4b). Plots with low HAN remained relatively healthy. Ash dieback severity also decreased with distance to the river (Table 1 and 2). Additionally, the crown dieback index significantly decreased with tree size (mean plot dbh) while canker prevalence increased with distance to the road (Table 2). The range of the spatial correlation was similar at the disease establishment and development stage and corresponds to 645 m for crown decline and 403 m for canker prevalence. The spatial effect showed similar patterns across the years (Fig. 5).

The fructification test showed that the visual assessment of rachis infection was valid. *Hymenoscyphus fraxineus* produced apothecia on very few of the rachides classified as non-infected (0.9%). When this occurred, apothecia were usually observed on a very short section of the rachis. By contrast, *H. fraxineus* produced apothecia on the majority of the rachides classified as infected (97%). The proportions of infected rachides observed in the litter were very high, at 70-75% in both 2016 and 2017 (range 20-100%), even in locations with little crown dieback (Fig. 2d). The proportion of infected rachides in the litter increased with host density (HAN) and proximity to the river (Table 2). By contrast, it was not significantly influenced by tree cover fragmentation, although it was marginally higher in forest settings than in agricultural

settings (Fig. 2d). The range of spatial correlation was of a similar order of magnitude compared to crown decline and collar canker prevalence at 352 m. The density of infected rachides in the litter is of special interest as it is a measure of the potential for inoculum production. The density of infected rachides per plot was highly variable, with median values of 8 and 14 $m.m^{-2}$ in 2016 and 2017 (range 0.2-60 $m.m^{-2}$, Fig. 2c). It increased with local host density (plot ash basal area, 0.03, confidence interval CI [0.01, 0.06]) and mean ash size (tree dbh, 0.02, CI [0.1, 0.04]). It was, however, not significantly related to any of the studied landscape features, in particular to tree cover fragmentation (parameter 2.2, CI [-0.5, 5.1]). The range in the density of infected rachides in the litter was similar in forest and agricultural settings (Fig. 2c). The number of apothecia per m of infected rachides in early July was 68 ± 14 in 2016, and 47 ± 17 in 2017. Apothecia abundance increased significantly close to the river and was higher in 2016 (both *p*-values < 0.01), but did not depend on tree cover fragmentation (*p*-value= 0.101). Hence, the amount of *H. fraxineus* apothecia per cm of infected rachis was similar in forest and in agricultural settings.

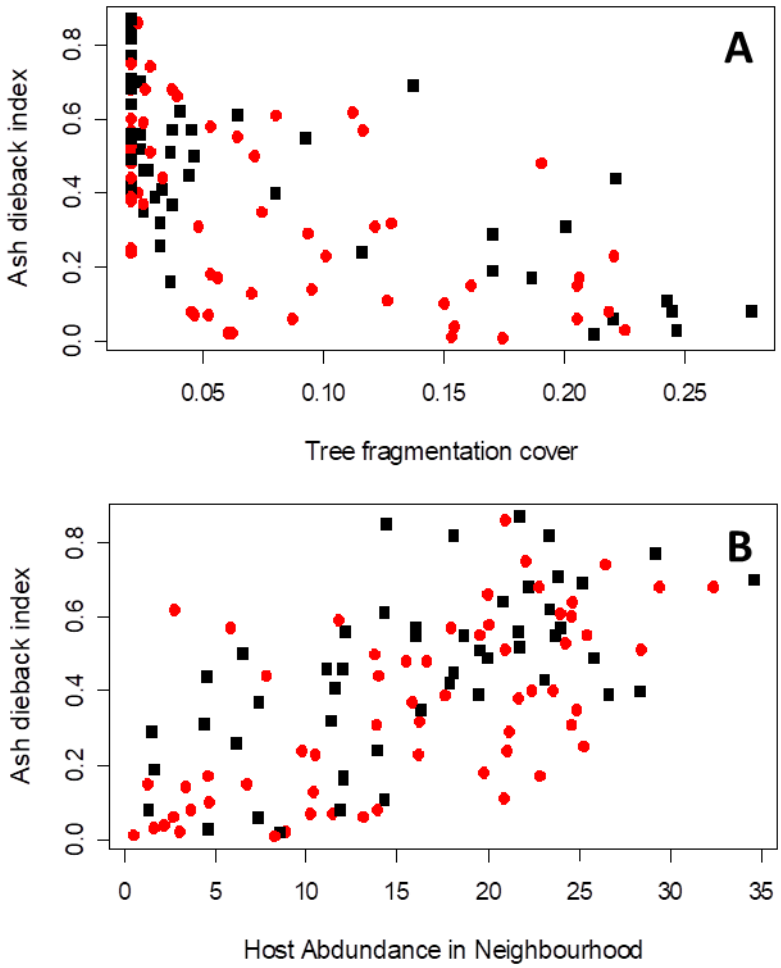

Fig. 4. Factor controlling the severity of ash dieback. Effect of (A) tree cover fragmentation and (B) host abundance in the neighbourhood (HAN) on the crown dieback index. The black squares represent sites with mean tree trunk diameter less than 15 cm while the red circles are those with mean tree trunk diameter over 15 cm.

Temperature modelling

Temperature in the crown of isolated trees in agricultural settings were higher than those of forest trees by 0.4°C on average, and remained above temperatures of 35°C for about 4 hours longer (p-value < 0.05). The height of the data logger in the crown did not influence the results (p-value = 0.34).

The model developed to explain hourly temperatures in the tree crown accounted for 91% of the variability observed (p-value < 0.01). Modelled temperatures were seldom higher than 35°C in 2016 and 2017 in both forest and agricultural settings (0 – 11h depending on the settings and the year). By contrast, modelled crown temperature were above 35°C for a total of 24 hours in 2015 in the forest and 64 hours in agricultural settings.

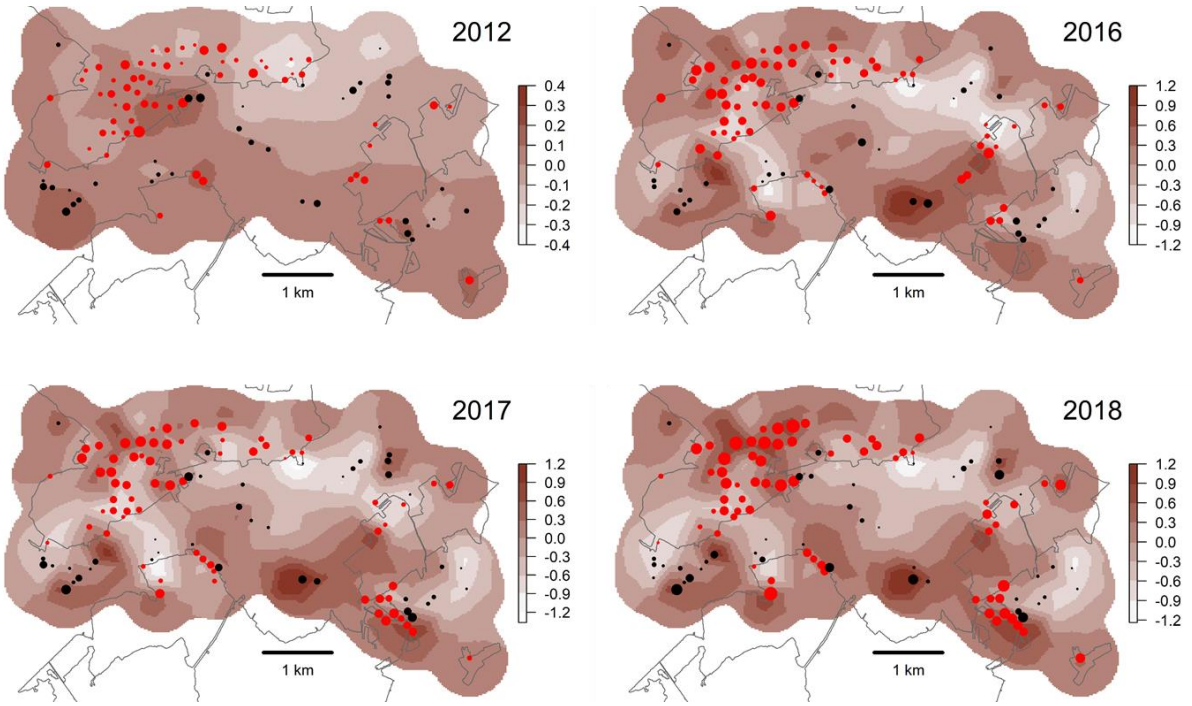

Fig. 5. Map of the posterior mean of the spatial random fields for ash dieback model for the disease establishment (2012) and development stage (2016-18). Red dots are forest settings while black dots are agricultural settings. Dots size corresponds to ash dieback severity. These maps show spatial effect that could not be explained by covariates of the model.

Discussion

Our results illustrate how landscape can affect the colonisation and subsequent development of an invasive disease in a new area. While initial colonisation was not strongly affected at the studied scale, several landscape features, in particular host density and tree cover fragmentation, were very important for the subsequent development of the disease. Furthermore, circumstantial evidence indicated that high summer temperatures may limit disease development, even in a temperate climate such as that of north-eastern France.

The colonisation of the studied area was very rapid, the pathogen being detected everywhere two years after it was first reported. Disease severity could not be related to potential dispersal corridors, such as tracks of dense host populations or roads and rivers that might have dispersed infected rachides. The relation between environmental heterogeneity, in particular host distribution, and the ability of a pathogen to invade an area have been well

documented both theoretically and empirically (Park *et al.,* 2001; Kauffmann & Jules, 2006; Condeso & Meentemeyer, 2007; Plantegenest *et al*., 2007; Laine & Hanski 2005). However, *H. fraxineus* has a very efficient airborne dispersal ability (Gross *et al.,* 2014), with a mean range for ascospores dispersal from inoculum sources as high as 1.5 to 2.5 km (Grosdidier *et al.,* 2018). The average distance between patches of ash in north-eastern France is likely to be lower, the species being frequent along roads and watercourses, in hedges and in forest settings. This was certainly the situation in the studied area. All patches of ash within the study area were already colonised in 2012 and remained so during the study period, despite the occurrence in 2015 of a heat wave that was unfavourablefor pathogen development. This is probably related to the ability of *H. fraxineus* to survive in infected rachides for several years (Kirisits, 2015), which gives some stability to the pathogen population. Some landscape features were related to the 2012 disease severity at the establishment stage (tree cover fragmentation and tree size). However, as they remained important throughout the studied period, it can be argued that they mostly influenced local disease intensification. Smaller ashes are already known to be more affected by *H. fraxineus* (Husson *et al.,* 2012; Skovsgaard *et al.,* 2017; Enderle *et al.,* 2018). The pattern of spatial correlation (spatial random fields for ash dieback model) observed in 2012 shows similarities with what was observed in later years, which might reflect patches of earlier colonisation by *H. fraxineus.* Alternatively, it could represent underlying environment heterogeneity not captured by the measured variables or heterogeneity in the resistance level of ash populations (McKinney *et al.,* 2014).

Although of little importance at the establishment stage, landscape features proved to be critical for subsequent disease development. In particular, we demonstrated the importance of host density for ash dieback. While considered critical in disease dynamics, this parameter has not often been documented for plant diseases affecting natural or semi-natural ecosystems (Plantegenest *et al*., 2007; Keesing *et al.,* 2010). Experimental work has demonstrated its importance in both grassland and trees systems (Knops *et al.,* 1999; Mitchell *et al.,* 2002; Borer *et al.,* 2009; Hantsch *et al*., 2013; Parker & Gilbert. 2018), but well documented empirical studies remain scarce (Haas *et al.,* 2011). However, host density dependent tree pathogens have been shown to promote diversity in tropical forests by maintaining individual species at low density, lowering the overall inter-species competition (Janzen-Connell hypothesis, Bever *et al.,* 2015). We showed that presence of large ash populations in the neighbourhood has an influence on ash dieback that decayed exponentially, but was still significant at 200-300 m. The index of host abundance used, HAN, can be seen as a surrogate for the force of infection: the density of infected ash rachides in the litter was strongly related to local host density and tree size, but not to the studied environmental parameters, while apothecia production on the infected rachides increased only in the vicinity of water courses. Thus, inoculum production depended mainly on the ash basal area. The range of the spatial dependency to neighbouring ash populations matches the range of ascospore dispersal (Grosdidier *et al.*, 2018). Although *H. fraxineus* ascospores can be detected up to 500 m from inoculum sources, the spore load in the air drops rapidly between 0 and 50 m. Analysis showed that incorporating HAN into the model did not account for all spatial dependency; some remained at a range of 300-600 m, which could partly reflect an incomplete measurement of ash density on the grid design. The strength of the host density effect may be explained by the disease etiology. *Hymenoscyphus fraxineu*s is a non-systemic pathogen and its spread in infected ash shoot tissues is usually about 10-20 cm (Gross *et al.*, 2014). It can thus be hypothesized that massive leaf infection is required to produce significant dieback. This may be even more relevant for collar cankers that appear to need large inoculum loads to occur (Marçais *et al.,* 2017). In fact, leaf infection appears to be massive: the proportion of infected rachides in the litter was usually very high (about 70%, with minimum values of 20%) and depended on host density and proximity to the river. The host density effect we demonstrated for ash dieback could be used to develop management strategies. We show that reducing the host density by promoting tree diversity in forest stands may be a valuable strategy to reduce their vulnerability to an invasive pathogen such as *H. fraxineus*. Forest invasive pathogens are currently increasing in frequency (Santini *et al.,* 2013). Moreover, they often involve pathogens not yet described and

thus remain difficult to predict. Promoting mixed forest stands could decrease their vulnerability to future potential invasive pathogens without targeting specific pathogenic species; this would be a way to adapt to this uncertainty.

Crown dieback and prevalence of collar canker induced by *H. fraxineus* were much more severe in forest than in agricultural settings. One of the reasons might be that ash density is usually lower in agricultural settings. However, foliar infection did not appear to be very different in forest and agricultural settings, suggesting that other mechanisms may explain the difference. The proportion of infected rachides in the litter might be a poor surrogate for leaf infection. Infected rachides have been shown to persist several years in the litter (Kirisits, 2015) and could decompose at different rates from non-infected rachides. Nevertheless, the potential for inoculum production was similar in forest and non-forest settings as neither infected rachis density in the litter nor production of apothecia per cm of infected rachis depended on tree cover fragmentation.

Alternatively, the difference between forest and agricultural settings could be related to micro-climatic conditions more favourable to *H. fraxineus* in forests. It is known that closed canopies create more humid and cool micro-climates (Villegas *et al.,* 2010), both conditions known to be favourable to leaf pathogens. Rosenvald *et al.* (2015) showed that trees at stand edges were less affected by *H. fraxineus* and hypothesized that high temperatures could limit disease development in these environments. Interestingly, in our work, crowns of isolated trees were more frequently exposed to temperatures above 35°C, which are very unfavourable for *H. fraxineus* survival (Hauptman *et al.,* 2013). Caution should, however, be taken with the data as we measured the crown temperature for only one year, which had a mild summer and the model we developed might thus inadequately take into account differences between forest and non-forest situations during a heat wave. It has also been shown that leaf temperatures can be above air temperatures by several degrees Celsius (Wiegand & Namken 1996). We additionally observed that high site moisture was also favourable to ash dieback: both crown dieback and inoculum production increased in proximity to rivers. This has already been reported by several authors (Husson *et al.,* 2012*;* Marçais *et al.,* 2016; Enderle *et al.*, 2018) and it has been hypothesized that dense stocking could favour disease severity by enhancing air humidity (Havrdová *et al.,* 2017).

Ash dieback has been reported to threaten the European ash population as well as some species that are closely associated with this tree species (Pautasso *et al.,* 2013, Mitchell *et al.,* 2014). We show here that this statement might be overly pessimistic. First, ash is frequently present within the landscape in sites where ash dieback remains mild, either because the tree canopy is open (isolated trees or hedges) or because ash is at low density in stands with mixed tree species. The overall disease severity should thus be mitigated at the landscape level. Secondly, heat waves appear to have limited disease severity in the studied area. With predicted global warming, the frequency of summer temperatures above 35°C is expected to increase in the area, which should reduce the impact of ash dieback. At the southern limit of ash dieback presence in France, Grosdidier *et al. (*2018) showed that the disease remains mild because summer temperatures are too high, with maximum daily air temperatures frequently reaching 35°C.

Acknowledgements

We thank Louis Cordonnier, Yann Guépet, Aurélie Backes, Pauline Hehn, Amrane Chabane-Chaouche, Anaïs Gillet and Olivier Caël for their technical assistance and the two anonymous reviewers that helped improve the manuscript. This work was supported by grants from the Forestry Health Department, French Ministry of Agriculture and Forestry and from ANSES. The UMR1136 and ANSES research units are supported by a grant managed by the French National Research Agency (ANR) as part of the "*Investissements d'Avenir*" program (ANR-11-LABX-0002-01, Laboratory of Excellence ARBRE).

Data Availability Statement

The data is available at Dryad with the doi: https://doi.org/10.5061/dryad.ns1rn8ppc

References

Bever, J. D., Mangan, S. A., & Alexander, H. M. (2015). Maintenance of Plant Species Diversity by Pathogens. *Annual Review of Ecology, Evolution, and Systematics*, *46*(1), 305–325. doi: 10.1146/annurev-ecolsys-112414-054306

Borer, E. T., Mitchell, C. E., Power, A. G., & Seabloom, E. W. (2009). Consumers indirectly increase infection risk in grassland food webs. *Proceedings of the National Academy of Sciences*, *106*(2), 503–506. doi: 10.1073/pnas.0808778106

Condeso, T. E., & Meentemeyer, R. K. (2007). Effects of Landscape Heterogeneity on the Emerging Forest Disease Sudden Oak Death. *Journal of Ecology* 95(2), 364-75. doi: 10.1111/j.1365-2745.2006.01206.x.

Enderle, R., Metzler, B., Riemer, U., & Kändler, G. (2018). Ash Dieback on Sample Points of the National Forest Inventory in South-Western Germany. *Forests*, *9*(1), 25. doi: 10.3390/f9010025

Grosdidier, M., Ioos, R., Husson, C., Cael, O., Scordia, T., & Marçais, B. (2018). Tracking the invasion: dispersal of Hymenoscyphus fraxineus airborne inoculum at different scales. *FEMS Microbiology Ecology*, *94*(5). doi: 10.1093/femsec/fiy049

Grosdidier, M., Ioos, R., & Marçais, B. (2018). Do higher summer temperatures restrict the dissemination of *Hymenoscyphus fraxineus* in France? *Forest Pathology*, e12426. doi: 10.1111/efp.12426

Gross, Andrin, Holdenrieder, O., Pautasso, M., Queloz, V., & Sieber, T. N. (2014). *Hymenoscyphus pseudoalbidus*, the causal agent of European ash dieback. *Molecular Plant Pathology*, *15*(1), 5–21. doi: 10.1111/mpp.12073

Guichard, S., & Augustin, S. (2002). Acute spread in France of an invasive pest, the horse chestnut leafminer Cameraria ohridellaDeschka & Dimic (Lep., Gracillariidae). *Anzeiger Fur Sch<html_ent Glyph="@auml;" Ascii="a"/>dlingskunde*, *75*(6), 145–149. doi: 10.1046/j.1439-0280.2002.02044.x

Haas, S. E., Hooten, M. B., Rizzo, D. M., & Meentemeyer, R. K. (2011). Forest species diversity reduces disease risk in a generalist plant pathogen invasion: Species diversity reduces disease risk. *Ecology Letters*, *14*(11), 1108–1116. doi: 10.1111/j.1461-0248.2011.01679.x

Hantsch, L., Braun, U., Scherer-Lorenzen, M., & Bruelheide, H. (2013). Species richness and species identity effects on occurrence of foliar fungal pathogens in a tree diversity experiment. *Ecosphere*, *4*(7), art81. doi: 10.1890/ES13-00103.1

Hauptman, T., Piškur, B., de Groot, M., Ogris, N., Ferlan, M., & Jurc, D. (2013). Temperature effect on *Chalara fraxinea* : heat treatment of saplings as a possible disease control method. *Forest Pathology*, *43*, 360–370. doi: 10.1111/efp.12038

Havrdová, L., Zahradnik, D., Romportl, D., Pešková, V., & Černý, K. (2017). Environmental and Silvicultural Characteristics Influencing the Extent of Ash Dieback in Forest Stands. *Baltic Forestry*, *23*, 168–182.

Havrdová, L., & Cerný, K. (2013). The importance of air humidity in ash dieback epidemiology–preliminary results. *Rep For Res*, *58*, 347–352.

Husson, C., Caël, O., Grandjean, J. P., Nageleisen, L. M., & Marçais, B. (2012). Occurrence of Hymenoscyphus pseudoalbidus on infected ash logs. *Plant Pathology*, *61*(5), 889–895. doi: 10.1111/j.1365-3059.2011.02578.x

Hutchinson, T. F., & Vankat, J. L. (1998). Landscape Structure and Spread of the Exotic Shrub Lonicera maackii (Amur honeysuckle) in Southwestern Ohio Forests. *The American Midland Naturalist*, *139*(2), 383–390. doi: 10.1674/0003-0031(1998)139[0383:LSASOT]2.0.CO;2

Ioos, R., Kowalski, T., Husson, C., & Holdenrieder, O. (2009). Rapid in planta detection of Chalara fraxinea by a real-time PCR assay using a dual-labelled probe. *European Journal of* Plant *Pathology*, 125(2), 329–335. doi: 10.1007/s10658-009-9471-x

Jules, E. S., Kauffman, M. J., Ritts, W. D., & Carroll, A. L. (2002). Spread of an invasive pathogen over a variable landscape: a nonnative root rot on port Orford cedar. *Ecology*, *83*(11), 3167–3181. doi: 10.1890/0012-9658(2002)083[3167:SOAIPO]2.0.CO;2

Jung, T., & Blaschke, M. (2004). Phytophthora root and collar rot of alders in Bavaria: distribution, modes of spread and possible management strategies. *Plant Pathology*, *53*(2), 197–208. doi: 10.1111/j.0032-0862.2004.00957.x

Kauffman, M. J., & Jules, E. S. (2006). Heterogeneity shapes invasion: Host size and environment influence susceptibility to a nonnative pathogen. *Ecological Applications*, *16*(1), 166–175. doi: 10.1890/05-0211

Keesing, F., Belden, L. K., Daszak, P., Dobson, A., Harvell, C. D., Holt, R. D., … Ostfeld, R. S. (2010). Impacts of biodiversity on the emergence and transmission of infectious diseases. *Nature*, *468*(7324), 647–652. doi: 10.1038/nature09575

Kelly, M., & Meentemeyer, R. K. (2002). Landscape dynamics of the spread of Sudden Oak Death. *Photogrammetric Engineering and Remote Sensing*, *68*, 1001–1009.

Kirisits, T. (2015). Ascocarp formation of *Hymenoscyphus fraxineus* on several-year-old pseudosclerotial leaf rachises of *Fraxinus excelsior*. *Forest Pathology*, *45*, 254–257. doi: 10.1111/efp.12183

Knops, J. M. H., Tilman, D., Haddad, N. M., Naeem, S., Mitchell, C. E., Haarstad, J., … Groth, J. (1999). Effects of plant species richness on invasion dynamics, disease outbreaks, insect abundances and diversity. *Ecology Letters*, *2*(5), 286–293. doi: 10.1046/j.1461-0248.1999.00083.x

Krewenka, K. M., Holzschuh, A., Tscharntke, T., & Dormann, C. F. (2011). Landscape elements as potential barriers and corridors for bees, wasps and parasitoids. *Biological Conservation*, *144*(6), 1816–1825. doi: 10.1016/j.biocon.2011.03.014

Laine, A.-L., & Hanski, I. (2006). Large-scale spatial dynamics of a specialist plant pathogen in a fragmented landscape. *Journal of Ecology*, *94*(1), 217–226. doi: 10.1111/j.1365-2745.2005.01075.x

Marçais, B., Husson, C., Cael, O., Dowkiw, A., Saintonge, F.-X., Delahaye, L., … Chandelier, A. (2017). Estimation of Ash Mortality Induced by Hymenoscyphus fraxineus in France and Belgium. *Balt. For*, *23*(1), 159–167.

Marçais, B., Husson, C., Godart, L., & Caël, O. (2016). Influence of site and stand factors on *Hymenoscyphus fraxineus* -induced basal lesions. *Plant Pathology*, *65*(9), 1452–1461. doi: 10.1111/ppa.12542

McKinney, L. V., Nielsen, L. R., Collinge, D. B., Thomsen, I. M., Hansen, J. K., & Kjaer, E. D. (2014). The ash dieback crisis: genetic variation in resistance can prove a long-term solution. *Plant Pathology*, *63*(3), 485–499. doi: 10.1111/ppa.12196

Meentemeyer, R. K., Haas, S. E., & Václavík, T. (2012). Landscape Epidemiology of Emerging Infectious Diseases in Natural and Human-Altered Ecosystems. *Annual Review of Phytopathology*, *50*(1), 379–402. doi: 10.1146/annurev-phyto-081211-172938

Mitchell, C. E., Tilman, D., & Groth, J. V. (2002). Effects of grassland plant species diversity, abundance, and composition on foliar fungal disease. *Ecology*, *83*(6), 1713–1726. doi: 10.1890/0012-9658(2002)083[1713:EOGPSD]2.0.CO;2

Mitchell, R. J., Beaton, J. K., Bellamy, P. E., Broome, A., Chetcuti, J., Eaton, S., … Woodward, S. (2014). Ash dieback in the UK: A review of the ecological and conservation implications and potential management options. *Biological Conservation*, *175*, 95–109. doi: 10.1016/j.biocon.2014.04.019

Park, A. W., Gubbins, S., & Gilligan, C. A. (2001). Invasion and persistence of plant parasites in a spatially structured host population. *Oikos*, *94*(1), 162–174.

Parker, I. M., & Gilbert, G. S. (2018). Density-dependent disease, life-history trade-offs, and the effect of leaf pathogens on a suite of co-occurring close relatives. *Journal of Ecology*, *106*(5), 1829–1838. doi: 10.1111/1365-2745.13024

Pautasso, M., Aas, G., Queloz, V., & Holdenrieder, O. (2013). European ash (Fraxinus excelsior) dieback – A conservation biology challenge. *Biological Conservation*, *158*, 37–49. doi: 10.1016/j.biocon.2012.08.026

Perkins, T. E., & Matlack, G. R. (2002). Human-generated pattern in commercial forests of southern Mississippi and consequences for the spread of pests and pathogens. *Forest Ecology and Management*, *157*(1–3), 143–154.

Plantegenest, M., Le May, C., & Fabre, F. (2007). Landscape epidemiology of plant diseases. *Journal of The Royal Society Interface*, *4*(16), 963–972. doi: 10.1098/rsif.2007.1114

R Core Team (2019). R: A language and environment for statistical computing. R Foundation for Statistical Computing, Vienna, Austria. URL https://www.R-project.org/.

Rodewald, A. D., & Arcese, P. (2016). Direct and Indirect Interactions between Landscape Structure and Invasive or Overabundant Species. *Current Landscape Ecology Reports*, *1*(1), 30–39. doi: 10.1007/s40823-016-0004-y

Rosenvald, R., Drenkhan, R., Riit, T., & Lõhmus, A. (2015). Towards silvicultural mitigation of the European ash (*Fraxinus excelsior*) dieback: the importance of acclimated trees in retention forestry [1]. *Canadian Journal of Forest Research*, *45*(9), 1206–1214. doi: 10.1139/cjfr-2014-0512

Santini, A., Ghelardini, L., De Pace, C., Desprez-Loustau, M. L., Capretti, P., Chandelier, A., … Stenlid, J. (2013). Biogeographical patterns and determinants of invasion by forest pathogens in Europe. *New Phytologist*, *197*(1), 238–250. doi: 10.1111/j.1469-8137.2012.04364.x

Schrödle, B., & Held, L. (2011). A primer on disease mapping and ecological regression using INLA. *Computational Statistics*, *26*(2), 241–258. doi: 10.1007/s00180-010-0208-2

Skovsgaard, J. P., Wilhelm, G. J., Thomsen, I. M., Metzler, B., Kirisits, T., Havrdová, L., … Clark, J. (2017). Silvicultural strategies for Fraxinus excelsior in response to dieback caused by Hymenoscyphus fraxineus. *Forestry: An International Journal of Forest Research*, *90*(4), 455–472. doi: 10.1093/forestry/cpx012

Turner, M. G. (2005). Landscape Ecology: What Is the State of the Science? *Annual Review of Ecology, Evolution, and Systematics*, *36*(1), 319–344. doi: 10.1146/annurev.ecolsys.36.102003.152614

Vacek, S., Vacek, Z., Bulusek, D., Putalova, T., Sarginci, M., Schwarz, O., … Moser, W. K. (2015). European Ash (Fraxinus excelsior L.) Dieback: Disintegrating forest in the

mountain protected areas, Czech Republic. *Austrian Journal of Forest Science. 4: 203-223.*, *4*, 203–223.

Villegas, J. C., Breshears, D. D., Zou, C. B., & Royer, P. D. (2010). Seasonally Pulsed Heterogeneity in Microclimate: Phenology and Cover Effects along Deciduous Grassland–Forest Continuum. *Vadose Zone Journal*, *9*(3), 537. doi: 10.2136/vzj2009.0032

Wiegand, C. L., & Namken, L. N. (1996). Influences of Plant Moisture Stress, Solar Radiation, and Air Temperature on Cotton Leaf Temperature1. *Agronomy Journal*, *58*(6), 582. doi: 10.2134/agronj1966.00021962005800060009x

Fig S1. Measurements taken and type of data collected in this paper.

Year	Data collected	Area	Nb sites observed	Nb trees observed
All years	Tree size (dbh)	All	127	2163
2012	Disease severity	All	100	1415
	Collar canker	All	100	1415
2014	Ash basal area	All	48	-
2016	Disease severity	All	100	1624
	Collar canker	All*	91	1443
	Density/ infection rachides in litter	All*	99	-
	Nb apothecia / m of infected rachides	Selection of plot in forest / agricultural settings	23	-
	Crown temperature	8 plots forest + 8 plots Hedges / Isolated trees	16	16
2017	Disease severity	All	109	1342
	Collar canker	All*	106	1243
	Density/ infection rachides in litter	All*	102	-
	Nb apothecia / m of infected rachides	Selection of plot in forest / agricultural settings	31	-
	Ash basal area	All	109	-
2018	Disease severity	All	111	1398
	Collar canker	All*	107	1165

*Some plots could not be observed for collar canker because of either accessibility or presence of urticating caterpillars